

# Continuous Fractionation of Fly Ash Particles by SPLITT for the Investigation of PCDD/Fs Levels in Different Sizes of Insoluble Particles

MYEONG HEE MOON,<sup>†</sup> DUKJIN KANG,<sup>†</sup> HEUNGBIN LIM,<sup>§</sup> JEONG-EUN OH,<sup>‡</sup> AND YOON-SEOK CHANG\*<sup>·‡</sup>

Department of Chemistry, Pusan National University, Pusan 609-735, Korea, Department of Chemistry, Dankook University, Seoul 140-714, Korea, and School of Environmental Science & Engineering, Pohang University of Science & Technology, Pohang 790-784, Korea

A combined analytical method has been developed to characterize the size dependent levels of polychlorinated dibenzo-*p*-dioxins (PCDDs) and polychlorinated dibenzofurans (PCDFs) contained in fly ash particles from a municipal solid waste incinerator (MSWI). Gravitational SPLITT fractionation (GSF), a relatively new technique for the fast and continuous separation of micron sized particles, was used to fractionate a fly ash sample, directly collected from a bag-filter house of MSWI in Korea, into six different size groups (<1.0, 1.0–2.5, 2.5–5.0, 5.0–10, 10–20, and 20–53  $\mu\text{m}$  in diameter) in water solution, and the resulting fractions are examined by high resolution gas chromatography/high resolution mass spectrometry (HRGC/HRMS) in order to determine the concentration of PCDD/Fs according to these particle sizes. The results from SPLITT fractionation show that approximately 54% of the fly ash particles (sieved fraction <53  $\mu\text{m}$ ) by weight have been found to be smaller than 5.0  $\mu\text{m}$  excluding the water soluble matter in the sample. From the HRGC/HRMS measurements, particle fractions in the size range of PM 1.0–2.5 and 2.5–5.0 appear to carry about 76 and 79 ng/g of PCDD/Fs which are relatively larger than those found in other diameter ranges. Principal component analysis (PCA) shows that particles larger than 5.0  $\mu\text{m}$  are clustered into a group predominantly containing low chlorinated dioxins and fractions smaller than 5.0  $\mu\text{m}$  into another group with lower chlorinated furans. This study demonstrated that the combining GSF with a secondary analytical method such as HRGC/HRMS has the potential to obtain size dependent information of particulate materials in relation to their production processes, chemical compositions, environmental fates, and other factors.

## Introduction

The main pathway of polychlorinated dibenzo-*p*-dioxins (PCDDs) and polychlorinated dibenzofurans (PCDFs) to enter the environment is known to be via combustion processes

(1–5). Among the environmental sources of PCDD/Fs, stationary plants such as municipal solid waste incinerators (MSWIs) have raised much concern since emission of such hazardous materials into the atmosphere results in the contamination of soils, plants, and water (1, 6). The potential impact on public health by emissions of PCDD/Fs has become a controversial issue since these materials can be directly inhaled by humans in the form of airborne gases and particles containing emissions or indirectly by ingestion of foods (plants and animals) produced near the facility (2, 7–9). Among the emission products of MSWIs, fly ash particles that are known to have a catalytic potential for the generation of PCDD/Fs during incineration processes (10, 11) play an important role in spreading the toxic materials over a wide region when they are released into the atmosphere. PCDD/Fs could be emitted not only from flue gas but also from fly ash collected by air pollution control devices and the waste management has largely dependent on landfilling (11).

To characterize the potential health effects of human exposure to fly ash particles emitted from incinerators or to study the formation/removal mechanism of PCDD/Fs during combustion processes, it is important to establish an analytical method to carry out hazardous identification with respect to the particle size of fly ash. Unfortunately, there has not been much work done to determine the size dependent distribution of pollutants contained in incinerator fly ash particles and few studies have focused on coarse particles size (above 37  $\mu\text{m}$  up to few hundreds) (12–14). In the literature, it has been reported that PCDD/Fs levels of fine atmospheric particles are higher than those of the large diameter range (15, 16). It is likely that fine particles of fly ash will have a stronger impact on human health, since lightweight fine particles can be spread over a wider area than heavy ones. Particles smaller than 10.0  $\mu\text{m}$  in diameter are well-known to have critical effects on human health when they are breathed (17, 18). Thus, it is important to determine a spectrum of hazardous materials according to fine particle size of fly ash by establishing a suitable and accurate analytical method.

To characterize the size dependent population of PCDD/Fs in fly ash particles, a considerable amount of sample particles is needed for each desired range of particle diameters. One gram or more of particles for each fraction is required. First of all, fly ash particles must be fractionated by size with a proper means. Current analytical techniques to fractionate colloidal or micron-sized particles by size are mostly limited by a small load capacity and are incapable of operating in a continuous mode. There are few preparative separation techniques such as mechanical sieving or gravity driven elutriation and air classification (19). However, the resolution of separation is limited due to the lack of an appropriate sieve for fine particles in the former technique and due to the nonuniform flow profile generated in the latter one. Cascade impactors (16) have been widely used for the collection of airborne particles with multistage size fractions, but their operation is limited to particles spread in the air.

Split-flow thin (SPLITT) fractionation, a new class of continuous separating techniques, has been developed into a rapid and accurate fractionating tool that is useful for colloids and particulate materials (20–25). A schematic view of SPLITT channel and the system configuration of gravitational SPLITT fractionation (or GSF) employing a gravitational force are shown in Figure 1. Separation in GSF is carried out in a thin, empty rectangular channel with the use

\* Corresponding author phone: 82 54 279 2281; fax: 82 54 279 8299; e-mail: yschang@postech.ac.kr.

<sup>†</sup> Pusan National University.

<sup>§</sup> Dankook University.

<sup>‡</sup> Pohang University of Science & Technology.

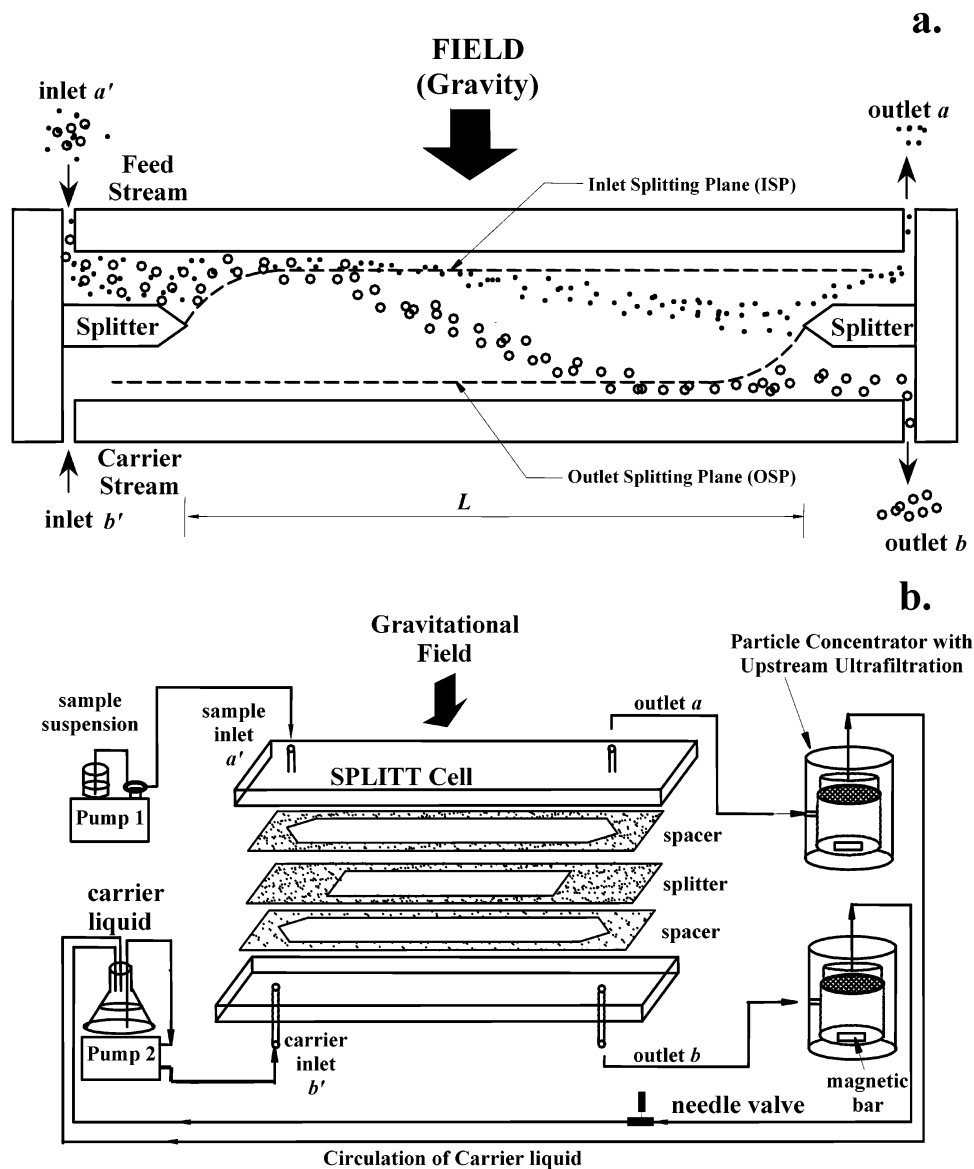


FIGURE 1. Schematics of gravitational SPLITT fractionation (GSF) channel (a) and the system configuration (b).

of two different streams of liquid flow. SPLITT channel is equipped with splitters that are designed to separate liquid flow streams, and the gravitational force is driven perpendicular to the axis of flow migration. In GSF, suspended sample particles are fed into the channel through the upper inlet  $a'$ , and, simultaneously, they are compressed toward the upper wall of the channel into a thin lamina by the fast moving carrier liquid introduced through inlet  $b'$  as shown in Figure 1a. The notation  $a'$  and  $b'$  denote each inlet of sample stream and carrier flow, respectively. While particles subjected to the upper wall of the channel are transported along the channel by the combined flow streams, the gravity causes them to settle according to mass or density of particles. Therefore, particles settling slowly will emerge from the upper outlet  $a$ , whereas the faster ones exit the lower outlet  $b$ . Eventually, fractions collected at both outlets contain particles larger than or smaller than a certain diameter range that is readily adjusted by regulating the two outlet flow rates.

The cutoff diameter,  $d_c$  in GSF is related to channel dimensions and flow rates employed by (24–26)

$$d_c = \sqrt{\frac{18\eta(\dot{V}(a) - 0.5\dot{V}(a'))}{bLG(\rho_p - \rho)}} \quad (1)$$

where  $\eta$  is the viscosity of carrier fluid,  $b$  is the channel breadth,  $L$  is the channel length,  $G$  is the gravitation,  $\rho_p$  is the particle density,  $\rho$  is the density of carrier fluid, and  $V$  is the volumetric flow rate of a particular substream denoted by the term within parentheses. By using eq 1, GSF can be used to remove oversized particles from polydisperse particulate materials. In addition, it can be used to isolate particles of a certain diameter range by performing a fractionation at  $d_c$  of an upper limit of the diameter range and then followed by a secondary fractionation at  $d_c$  of a lower diameter limit. By accomplishing a series of fractionations at increasingly smaller cutoff diameters, a polydisperse particulate sample can be separated into various fractions. Since separation in GSF is performed in a continuous mode, the capacity to separate fly ash particles can be expanded into few gram scales at various diameter ranges.

In the current work, GSF and HRGC/HRMS are combined for the study of PCDD/Fs levels in fly ash from MSWI according to particle sizes. The fly ash sample is not an aerosol type but an original ash sample collected from a bag-filter house of incinerator. The advantages of the joint use are because the GSF is effective at separating fly ash particles into different size fractions in preparative scales (~gram scale) and the HRGC/HRMS is effective in determining PCDDs and

PCDFs contained in each fraction. The aim of this study is to establish an analytical procedure for characterizing toxic waste products related to particle sizes and their distributions, which can be applied to micrometer sized environmental particulates. For an efficient separation of fly ash particles in GSF, a slow-flow sample-feed method is utilized after an initial fractionation, roughly made at a relatively high speed for each size fraction. During bulk, continuous fractionations of fly ash particles, PCUU (particle concentrator with upstream ultrafiltration) (25), is utilized online to isolate collected particles and to circulate carrier solution. The examined fly ash particle sample is fractionated into six different size fractions (<1.0, 1.0–2.5, 2.5–5.0, 5.0–10, 10–20, and 20–53  $\mu\text{m}$ ) by GSF, and the insoluble particle size of each fraction is confirmed by optical and electron microscopic measurements. Resulting fractions are examined for their concentrations and homologue patterns of PCDDs and PCDFs with the relative distribution.

## Experimental Section

**Sample Preparation.** The fly ash sample collected from a MSWI in Changwon, Korea was dried in an oven at 105 °C for 2 h. The type of incinerator was a stoker (200 ton/day)–boiler–spray dryer reactor–bag filter–stack and the incineration temperature was 850–900 °C. About 100.0 g of dried fly ash sample was initially treated with a 270-mesh sieve (~53- $\mu\text{m}$  in pore) in wet conditions, and the fly ash fraction smaller than 53- $\mu\text{m}$  was used for SPLITT fractionation. Wet sieving of a 100.0 g of dried fly ash particles provides 3.55 g of the fraction L (>53  $\mu\text{m}$ ) and 51.57 g of the fraction S (<53  $\mu\text{m}$ ), and the rest of the materials were presumed to dissolve in the solution, which was prepared with ultrapure water (> 18 M $\Omega$ ) containing 0.02% NaN<sub>3</sub> as a bactericide. Therefore, since approximately 45% of solid particles were dissolved in the solution, this work focused on fractionating only insoluble particles by SPLITT fractionation. After sieving, the solution was filtered through a membrane filter having a pore size of 0.2  $\mu\text{m}$ . Filtered fine particles were added to the fraction S for SPLITT fractionation, and the filtered solution was diluted into about total 5 L of 0.02% NaN<sub>3</sub> solution which was utilized as a carrier solution in GSF. At the end of SPLITT processes, 1 L of the carrier solution was taken for dioxin analysis.

**SPLITT Fractionation.** The GSF system used in this study was built with acrylic blocks in the laboratory. The system assembly is illustrated in Figure 1b. Five different channels were used for the consecutive SPLITT fractionations according to the various cutoff diameters. All channels are equally thick, 360- $\mu\text{m}$ , which is the total thickness of two 130- $\mu\text{m}$  thick Mylar spacers with one 100- $\mu\text{m}$  thick stainless steel plate used as splitters. The five channels have different breadths, *b*, and lengths, *L*. The dimensions are 2  $\times$  5 cm (*b* $\times$ *L*) for channel I, 2  $\times$  10 for channel II, 3  $\times$  15 for channel III, 4  $\times$  20 for channel IV, and 6  $\times$  20 for channel V. The construction of SPLITT channel is explained in an earlier publication (25).

Approximately 30.0 g of fraction S of the fly ash sample were dispersed with a concentration of about 1.0% (w/v) in the same carrier solution prepared at the above. Suspended particles were fed into a GSF channel through the inlet *a'* via a peristaltic pump from Gilson (Villers-le-Vel, France). The carrier liquid was delivered to the inlet *b'* by an FMI lab pump from Fluid Metering, Inc. (Oysterbay, NY). Two PCUUs were employed at channel outlets in order to concentrate the particle solution online during GSF runs as explained in an earlier work (25), and a fine metering valve from Crawford Fitting Co. (Solon, OH) was located at the outlet of a PCUU that was connected to channel outlet *b* for the accurate control of flow rates. The system assembly is illustrated in Figure 1b. The membrane material used inside the PCUU was 47 mm (in diameter) cellulose having a pore size of 1.2

$\mu\text{m}$ . While the particles were being concentrated in PCUU, they were stirred magnetically to produce a tangential flow that is helpful in keeping the membrane pores from being blocked. The filtrate solution passed through each PCUU was forwarded to the carrier reservoir for circulation. Since PCUU utilized upstream flow filtration, it was helpful to collect particles without inducing a serious blockage of membrane surface that may have occurred in a typical downstream filtration. Final particle fractions were dried in an oven for 2 h and were kept in vials. Collected particle fractions were examined either by a CSB-HP3 optical microscope from Samwon Scientific Ind. Co. (Seoul, Korea) or by S-4200 Scanning Electron Microscope from Hitachi Ltd. (Tokyo, Japan).

**Dioxin Analysis.** Sample preparation for the analysis of PCDD/Fs was accomplished according to the US EPA method 1613. About 1 g of each dried fly ash fraction collected from SPLITT fractionation was transferred to glass Soxhlet thimbles, spiked with a mixture of <sup>13</sup>C<sub>12</sub>-labeled PCDD/Fs internal standards (1 ng) and extracted for 16 h with toluene. To check any dissolved dioxins in the carrier solution used for GSF runs, 2 L of carrier solution was extracted with toluene after spiking the internal standards (1 ng). The extracts were washed with H<sub>2</sub>SO<sub>4</sub> until colorless and then with hexane followed by a water rinse for neutralization. Sample cleanup is carried out in two stages: (a) silica gel column (with layers of basic, neutral, acidic, and neutral silica) and (b) activated acidic alumina column capped with anhydrous Na<sub>2</sub>SO<sub>4</sub> and concentrated with N<sub>2</sub> gas. Before mass analysis, <sup>13</sup>C<sub>12</sub>-labeled PCDD/Fs-recovery standards (1 ng) were added.

PCDD/Fs were analyzed by utilizing a high-resolution gas chromatography/high-resolution mass spectrometry (HRGC/HRMS: HP 6890 series II/JMS 700T) with a DB-5MS column (60-m in length, 0.25-mm in i.d., 0.25- $\mu\text{m}$  in film thickness). The temperature program of a HRGC run was as follows: (1) initial isothermal hold at 140 °C for 4 min, (2) increased by 15 °C/min to an isothermal hold at 220 °C for 3 min, (3) increased by 1.5 °C/min to an isothermal hold at 240 °C for 2 min, and (4) increased by 4 °C/min to an isothermal hold at 310 °C for 6 min. The sample was introduced by splitless injection. The MS was operated at 10 000 resolution under positive EI conditions (38 eV electron energy), and data were obtained in the single ion monitoring (SIM) mode. Two ions among *M*<sup>+</sup>, *M* + 2, and *M* + 4 were monitored. The toxic 2,3,7,8 substituted PCDD/Fs were quantified as well as the totals for the tetra to octa-chlorinated homologues based on the following criteria: (1) isotope ratios within  $\pm 15\%$  of theoretical values and (2) signal-to-noise ratio  $\geq 2.5$ . Recoveries of the <sup>13</sup>C<sub>12</sub>-labeled PCDD/Fs-internal standards in the environmental samples were in the range of 50–120% which meets EPA method 1613 protocols.

## Results and Discussion

This study focused on demonstrating a combined analytical method to determine PCDD/Fs levels for insoluble fly ash particles fractionated at a different range of diameters. To obtain particle fractions of different diameters, the sieve fraction S (<53 $\mu\text{m}$ ) of fly ash particles was first dispersed in water and then separated into six different fractions of different diameters using a gravitational SPLITT fractionation (GSF) technique. The diameters were in these ranges: 53–20, 20–10, 10–5.0, 5.0–2.5, 2.5–1.0, and <1.0  $\mu\text{m}$ . Since at least 1 g of each particle fraction is needed for the analysis of PCDD/Fs, sufficient amount of the fraction S is provided to put in for the initial GSF run. To efficiently separate the bulk amounts of fly ash particles in GSF, several factors were studied in the previous work (25): the effect of sample feed rate and concentration on the percent recovery of particles at a desired diameter range. It is likely that repeating the separation method will increase the percent of particles

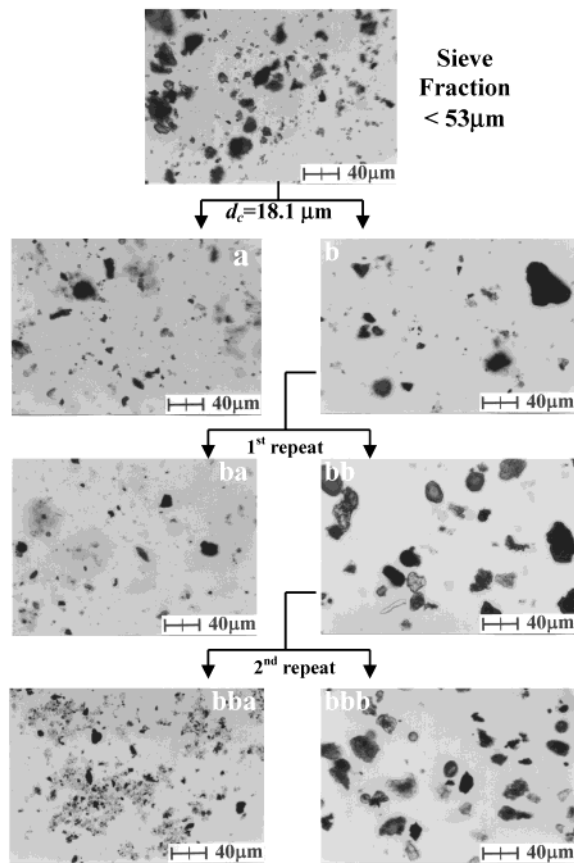


FIGURE 2. Optical micrographs of results from the repeated GSF runs for the sieve fraction S (<math>< 53 \mu\text{m}</math>).

recovered for each fraction smaller and larger than  $d_c$ . For the test of repeat effect, the fraction S (<math>< 53 \mu\text{m}</math>) is subjected to GSF for a cutoff diameter of  $18.1 \mu\text{m}$  by using channel II ( $2 \times 10 \text{ cm}$ ). Experimental flow rates for each inlet and outlet are  $\dot{V}(a') = \dot{V}(b) = 4.0 \text{ mL/min}$  and  $\dot{V}(b') = \dot{V}(a) = 34.0 \text{ mL/min}$ . The SPLITT fractionation schemes for the repeat runs are shown in Figure 2 as optical micrographs of fractions collected at each outlet. The SPLITT fractionation of the fraction S provides two fractions a and b marked in the micrographs. The notations a and b follow the symbol of each channel outlet. The fraction a is expected to contain particles smaller than  $d_c (= 18.1 \mu\text{m})$  and the fraction b larger than  $d_c$ . Micrographic examination of the fraction a shows that the percent recovery smaller than the cutoff diameter reaches more than 95% of the number of particles. However, the fraction b shows a poor recovery percentage. It contains numerous small particles present since the particle suspension fed into GSF was relatively concentrated as 2% which is relatively high for the feed rate,  $4.0 \text{ mL/min}$ . The same fractionation run is repeated for the fraction b under the same run condition, and the subsequent fractions denoted as ba and bb show percent recoveries of approximately 99% and 44%, respectively. In the first repeated run, there are still a large number of small particles (mostly smaller than  $5 \mu\text{m}$ ) eluted through outlet b. A further fractionation of the fraction bb results in an increase in the percent of particles recovered for the fraction bbb about 70%. Repeated runs can improve the separation efficiency to some degree, but this effect is no greater than can be obtained by using a diluted sample suspension or by using a reduced feed rate as found in an earlier work (25). Based on this observation, bulk fractionation of fly ash particles was first carried out at a relatively fast feed rate in order to achieve a given cutoff diameter, and then the collected fraction was fractionated at a reduced feed rate in

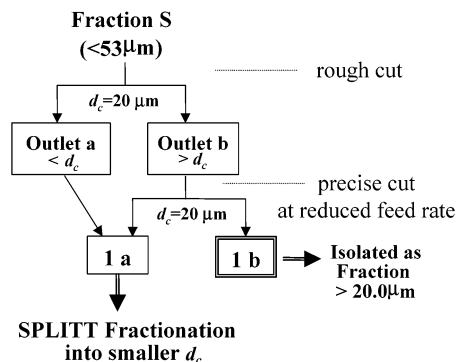


FIGURE 3. Schemes of gravitational SPLITT cell separation of the fraction S at a cutoff diameter  $d_c = 20 \mu\text{m}$ . Initial cut is made roughly and followed by a precise cut at a reduced feed rate. Fraction 1a is reused for fractionation at smaller cutoff diameters.

order to improve separation resolution. Both fractionation runs are adjusted to give an identical cutoff diameter by adjusting flow rates. This procedure is applied for all particle size fractionation steps hereafter.

For the fractionation of fly ash particles into different diameter groups, about  $30.0 \text{ g}$  of the fraction S (<math>< 53 \mu\text{m}</math>) was subjected to GSF for a series of fractionations at several cutoff diameters ( $d_c = 20, 10, 5.0, 2.5, \text{ and } 1.0 \mu\text{m}$ ). The experimental scheme for the first fractionation at a cutoff diameter of  $d_c = 20 \mu\text{m}$  is shown in Figure 3. The initial fractionation is a rough cut with  $1.0\%$  (w/v) particle suspension at the relatively fast feed flow rate,  $\dot{V}(a')$ , of  $4.0 \text{ mL/min}$  and the carrier flow rate,  $\dot{V}(b)$ , of  $21.6 \text{ mL/min}$  using channel I. Outflow rates are adjusted so that  $\dot{V}(a) = \dot{V}(b)$  and  $\dot{V}(b) = \dot{V}(a')$ . This rough fractionation will isolate most of large particles ( $> 20 \mu\text{m}$ ) with a number of small size particles left in the fraction that is collected at the lower outlet b of the SPLITT channel. Once the rough fractionation is made, a more precise cut is made using the fraction obtained at outlet b in order to remove the remaining undersized particles ( $< 20.0 \mu\text{m}$ ) at the reduced feed rate,  $\dot{V}(a')$ , of  $2.0 \text{ mL/min}$  with  $\dot{V}(b') = 20.6 \text{ mL/min}$ . The latter is adjusted in such a way to yield a  $d_c$  identical to that of the initial run according to eq 1. Even though both run conditions yield the same cutoff diameter, they are different in the precision of separation. From SPLITT calculation, it is known that particles of a certain diameter interval around  $d_c$  elute at both outlets under a given flow rate condition. For the above case, the smallest diameter eluted at outlet b,  $d_{bs}$  (26), during the second run is calculated as  $19.5 \mu\text{m}$  which is larger than the value ( $19.0 \mu\text{m}$ ) for the first run condition. Thus, particles smaller than  $20 \mu\text{m}$  can further be depleted from the fraction collected at the outlet b by using a reduced feed rate. The calculated  $d_c$ ,  $d_{bs}$ , and  $d_{al}$  (the largest diameter eluted at outlet a) at each fractionation step are listed in Table 1 along with experimental flow rate conditions. The particle fractions finally collected at the first stage of fractionation ( $d_c = 20 \mu\text{m}$ ) are named fraction 1a and 1b, in which the number denotes the stage of cutoff level and a represents the outlet that is collected from. The micrographs of both fractions are shown in Figure 4. While fraction 1b, which is expected to contain particles larger than  $20 \mu\text{m}$ , is saved for the dioxin analysis, fraction 1a having particles smaller than  $20 \mu\text{m}$  is used for the second fractionation stage ( $d_c = 10 \mu\text{m}$ ).

Normally, feeding at a slow flow rate with a diluted particle suspension will lower the rate of throughput, which results in an increased separation time. When a large cutoff diameter is fractionated, GSF requires a high speed flow as observed in the first stage of fractionation in Figure 4. Either of the cases will end up with a significant amount of particle solution that must be removed for the isolation of particulate matter.

**TABLE 1. Experimental Conditions for Gravitational SPLITT Fractionation of the Fly Ash According to Each Cutoff Diameter,  $d_c^a$**

$d_c$ ( $\mu\text{m}$ )	$\dot{V}(a')$ (mL/min)	$\dot{V}(b')$ (mL/min)	$\dot{V}(a)$ (mL/min)	$\dot{V}(b)$ (mL/min)	$d_{a'}-d_{b'}$ ( $\mu\text{m}$ )	channel systems ( $b \times L$ in cm)
20.0	4.0	21.6	21.6	4.0	21.0–19.0	I ( $2 \times 5$ )
	2.0	20.6	20.6	2.0	20.5–19.5	
10.0	4.0	24.1	24.1	4.0	10.5–9.5	III ( $3 \times 15$ )
	2.0	23.1	23.1	2.0	10.2–9.8	
5.0	4.0	11.8	11.8	4.0	5.5–4.5	IV ( $4 \times 20$ )
	1.0	10.3	10.3	1.0	5.1–4.9	
2.5	2.0	4.7	4.7	2.0	2.8–2.2	V ( $6 \times 20$ )
	1.0	4.2	4.2	1.0	2.7–2.3	
1.0	0.4	0.8	0.8	0.4	1.2–0.8	V

<sup>a</sup> The flow rates and channel dimensions are listed. At each cut off diameter condition, a rough fractionation is preceded with a relatively high feed rate, and then a reduced feed rate is used to improve the recovery rate for the collected fraction.

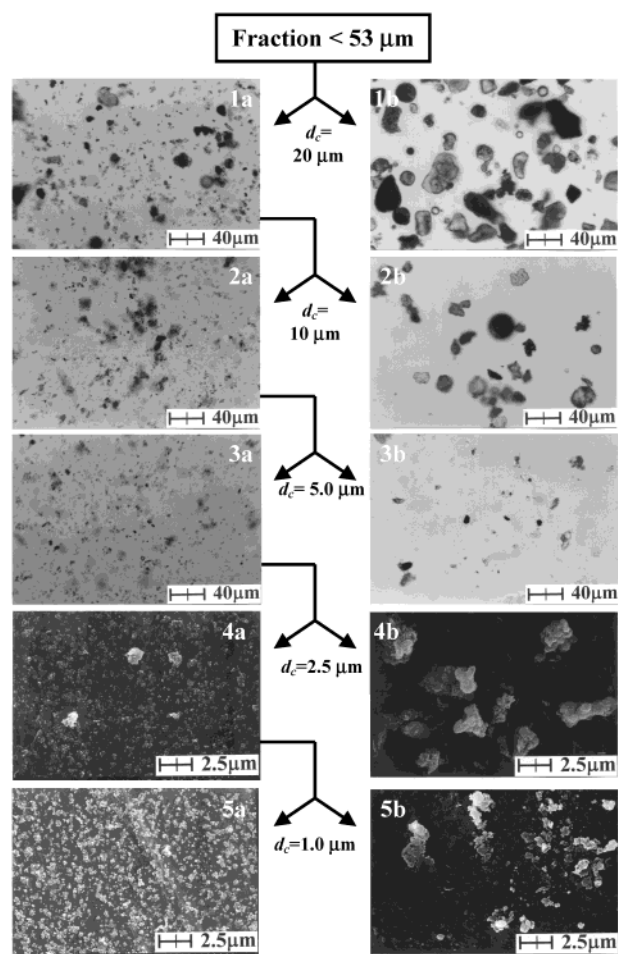


**FIGURE 4. Optical micrographs (1a–3b) and SEM pictures (4a–5b) results from the repeated GSF runs of fly ash particles ( $> 53 \mu\text{m}$ ) at five different cutoff diameters. The diameter ranges expected from SPLITT calculation are 20–53  $\mu\text{m}$  for the fraction 1b, 10–20  $\mu\text{m}$  for 2b, 5–10  $\mu\text{m}$  for 3b, 2.5–5.0  $\mu\text{m}$  for 4b, 1.0–2.5  $\mu\text{m}$  for 5b, and  $< 1.0 \mu\text{m}$  for 5a.**

The isolation of solid particles from the solution collected at both outlets of a SPLITT channel is necessary either for further fractionation at smaller cutoff diameters or for the secondary chemical or physical analysis of collected particles. Conventional GSF operation requires a centrifugation of particle solution collected at both outlets, and this process can be a time consuming step when fractionating bulk amounts and

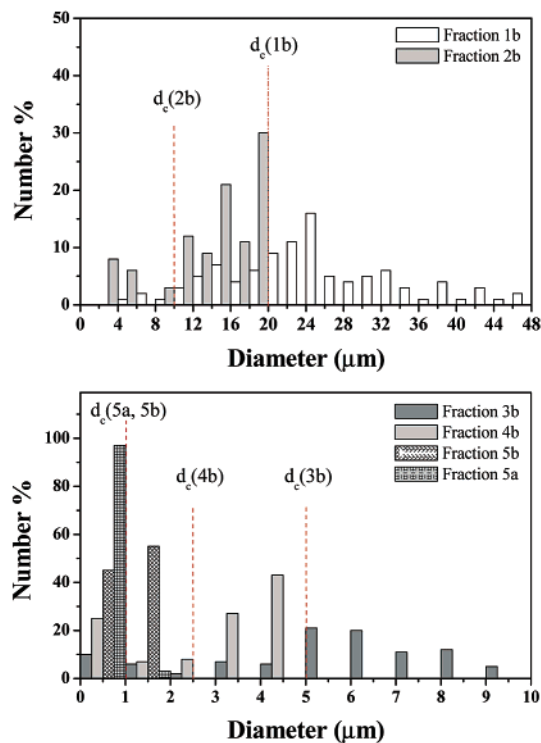


**FIGURE 5. Number distribution of particles in six fractions marked with each cutoff diameter. Measurements are made from 400–500 particles of each micrograph.**

for a series of fractionations into different cutoff diameters. In this work, a PCUU is employed for the online concentration of particles by connecting to each outlet of a SPLITT channel as shown in Figure 1b. The advantages of using PCUU are the concentration of collected particles right after exiting each outlet and then circulating the filtrate solution to the carrier liquid for reuse. This eliminates the necessity of using a centrifuge to reduce the amount of carrier liquid. Another important factor in using PCUU is the accuracy with which outlet flow rates can be controlled. This is done by connecting a needle valve after PCUU of outlet b. Since cutoff diameter of SPLITT fractionation is affected critically by the experimental flow rates as seen in eq 1, flow rates need to be controlled accurately. The first stage of fractionation at  $d_c = 20 \mu\text{m}$  requires a feed of 3.0 L of particle suspension, which will create about 15.7 L of particle solution only for fraction 1a at a rough cut without PCUU. Thus, using PCUU greatly reduces time and effort needed to concentrate the collected particle solution during the fractionation of a large amount of fly ash, and it was utilized for the subsequent GSF runs for smaller cutoff diameters.

The next cutoff diameter of 10  $\mu\text{m}$  was fractionated for fraction 1a with channel III. The flow rate conditions for both rough and precise cuts are listed in Table 1. As the cutoff diameters become smaller, different channel dimensions were used to provide a migration path long enough to allow for a good separation of small particle fractions. The resulting fraction, 2b, is expected to have particles within the size range of 10–20  $\mu\text{m}$ . Further fractionations were made in similar ways at cutoff diameters of 5, 2.5, and 1.0  $\mu\text{m}$  which resulted in the collection of fractions 3b (5.0–10  $\mu\text{m}$ ), 4b (2.5–5.0  $\mu\text{m}$ ), 5b (1.0–2.5  $\mu\text{m}$ ), and 5a ( $< 1.0 \mu\text{m}$ ). Each experimental condition is listed in Table 1. The collected fractions were examined microscopically in order to count the number of particles within the diameter range expected in each fraction. The resulting size distributions are represented with graphs in Figure 5. Measurements of particles were made with more than 400 particles of each fraction.

**TABLE 2. PCDD/Fs Concentration of Each Size Fraction of Fly Ash Samples from MSWI<sup>a</sup>**

sample/fraction no.	diameter range ( $\mu\text{m}$ )	wt (g)	local wt percent	total adjusted wt percent	PCDD/Fs concentration	
					TEQ (ng I-TEQ/g)	total (ng/g)
raw fly ash		100.00		100.00	0.17	14.65
dissolved matters <sup>b</sup>	in carrier solution	44.88		44.88	0.001 <sup>1</sup>	0.02 (ng/L)
sieve fraction L	>53	3.55		3.55	0.26	57.25
sieve fraction S	<53	51.57				
<b>Gravitational SPLITT Fractionation of Sieve Fraction S</b>						
GSF for sieve fraction S	<53	30.00	100.0			
GSF fraction 1b	20–53	1.35	4.5	2.32	0.10	9.28
GSF fraction 2b	10–20	3.20	10.6	5.50	0.12	20.91
GSF fraction 3b	5.0–10	5.53	18.4	9.51	0.46	48.16
GSF fraction 4b	2.5–5.0	12.23	40.8	21.02	1.11	79.10
GSF fraction 5b	1.0–2.5	2.99	10.0	5.14	1.12	76.77
GSF fraction 5a	<1.0	1.05	3.4	1.75	0.68	47.70
loss during GSF <sup>c</sup>		3.68	12.3	6.33		

<sup>a</sup> Fractions are first obtained by the sieving technique at 53  $\mu\text{m}$  and then followed by a series of gravitational SPLITT fractionation works.

<sup>b</sup> Soluble matters dissolved in water during sieving that is used for GSF. <sup>c</sup> These are expected to be from dissolution during GSF and are included into the dissolved matters (see footnote *b*) for PCDD/Fs analysis.

Fraction 1b in Figure 5 shows that more than 70% of particles are larger than  $d_c$  ( $=20 \mu\text{m}$ ), whereas fraction 2b shows more than 85% of particles are within the expected size range. A large deviation in fraction 1b may be because of a variation in the density of particles and the effect of their shapes since large fly ash particles ( $>20 \mu\text{m}$ ) appear to vary more in their shapes than the smaller diameter particles do. Since spherical particles agree well with SPLITT fractionation theory, the irregular shape of the large particles results in a result of the change of sedimentation coefficient leading to an actual cut-off diameter deviated from a calculated one. However, the effect of shape is not considered in this calculation since information on the aspect ratio of these particles is not clearly known.

Table 2 lists the weight of each dried fraction and the percentage of the total weight each diameter interval contributes. In Table 2, approximately 54% of the fraction S ( $<53 \mu\text{m}$ ) by weight, excluding lost particles during GSF runs, appears to be smaller than 5.0  $\mu\text{m}$ , and this is equivalent to about 28% of the raw fly ash particles including soluble parts. Especially, it shows that a largest population falls in the PM 2.5–5.0 in the fly ash sample produced by a MSWI located in Korea. Weight loss during GSF is presumed to be from soluble parts dissolved further or from very tiny particles that passed through the membrane filter (0.1  $\mu\text{m}$  pore size) since the carrier solution used for all of the GSF runs was filtered in order to retrieve the residual particles. The residual particles are added to fraction 5a ( $<1.0 \mu\text{m}$ ).

Table 2 lists the concentration of PCDD/Fs in the raw fly ash, the seven fractions, and the filtered solution. The concentrations of PCDD/Fs for each fraction ranged from 9.28 to 79.10 ng/g (0.10–0.12 ng I-TEQ/g-fraction). Since the carrier liquid used for GSF has been shown to contain a very low level of PCDD/Fs, as low as 0.02 ng/L, the possibility of losing fine particles into the solution is rather small, and further dissolution of soluble matter could occur during GSF. Since the measurement for the carrier liquid is based on 1 L out of a total of 5 L, the data represent for PCDD/Fs concentration of the dissolved matters contained in about 20 g of original fly ash particles. Upon comparing the relative abundance of PCDD/Fs at each fraction, it shows that the fractions 1.0–2.5 and 2.5–5.0  $\mu\text{m}$  have the largest concentrations of about 76 and 79 ng/g, respectively. This result strongly suggests that PCDD/Fs are preferentially carried on particles smaller than 5.0  $\mu\text{m}$ . According to the reports by Chang (12), Clement (13), and Karasek (14), a similar trend has been reported as the concentration of PCDD/Fs increases

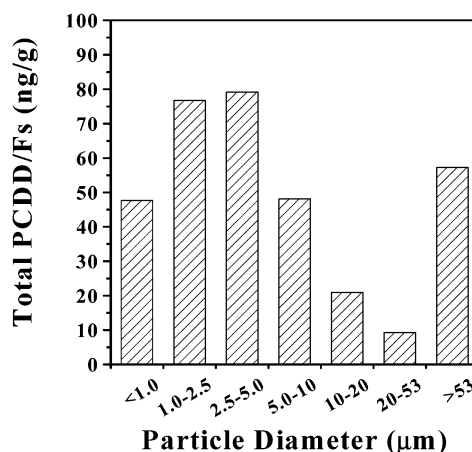


**FIGURE 6. Total PCDD/Fs concentration ( $\mu\text{g/g}$ ) vs particle size range.**

with the decrease of particle size of fly ash. However, these observations are mostly focused on coarse particles up to a several hundred  $\mu\text{m}$  without a fine fractionation of particles smaller than 37  $\mu\text{m}$ . Since there has been no close consideration as fine as those illustrated in this study, the joined method (GSF-HRGC/HRMS) could be a potential analytical tool for monitoring these pollutants contained in fine particle size regimes.

Figure 6 shows the plot of the concentrations of PCDD/Fs vs particle size. Apparently, PM 1.0–2.5 and 2.5–5.0 of fly ash fractions seem to carry PCDD/Fs exclusively compared to other diameter ranges examined in this study. The concentrations of PCDD/Fs homologues measured in each size fraction are listed in Table 3, and their homologue patterns are compared by normalizing the data to the sum of [PCDDs] + [PCDFs] = 1 in Figure 7. Due to the large variation in PCDD/Fs homologue patterns in Figure 7, a distinguishing difference in the pattern based on particle size is not likely. However, it seems like that particles larger than 5.0  $\mu\text{m}$  have PCDDs distributions somewhat larger than those of the smaller ones but are relatively small in case of PCDFs. Therefore, principal component analysis (PCA) was used to make sure of similarities or differences of PCDD/Fs homologue patterns. Figure 8 (a) shows the loading plot of PCA indicating that the two significant components account for 87% (69% + 18%) of the variation among the data. The principal component 2 (P[2]) divides all particle size fractions into two distinguished groups except one fraction ( $>53 \mu\text{m}$ ).

TABLE 3. Concentration of PCDD/Fs in Various Size Fractions of Fly Ash Particles from MSWI

fractions isomer	raw fly ash	(ng/g)							dissolved matters in carrier solution (ng/L)
		>53 $\mu\text{m}$	53–20 $\mu\text{m}$	20–10 $\mu\text{m}$	10–5 $\mu\text{m}$	5–2.5 $\mu\text{m}$	2.5–1.0 $\mu\text{m}$	<1.0 $\mu\text{m}$	
2378-TCDD	0.010	0.022	0.005	0.007	0.023	0.058	0.057	0.034	0.000
12378-PeCDD	0.043	0.069	0.024	0.022	0.092	0.208	0.193	0.116	0.000
123478-HxCDD	0.037	0.080	0.019	0.035	0.106	0.194	0.228	0.142	0.000
123678-HxCDD	0.049	0.136	0.038	0.088	0.227	0.445	0.414	0.257	0.000
123789-HxCDD	0.030	0.181	0.019	0.042	0.107	0.212	0.253	0.150	0.000
1234678-HpCDD	0.479	0.998	0.223	0.681	1.523	2.873	2.925	1.603	0.000
OCDD	2.145	3.814	0.984	3.404	6.220	10.692	10.296	5.596	0.002
2378-TCDF	0.059	0.103	0.037	0.031	0.138	0.342	0.307	0.185	0.001
12378-PeCDF	0.089	0.177	0.049	0.046	0.223	0.555	0.590	0.370	0.001
23478-PeCDF	0.126	0.253	0.079	0.076	0.332	0.865	0.851	0.514	0.001
123478-HxCDF	0.110	0.202	0.065	0.060	0.272	0.756	0.721	0.443	0.001
123678-HxCDF	0.127	0.269	0.073	0.070	0.330	0.824	0.951	0.581	0.000
234678-HxCDF	0.168	0.343	0.092	0.094	0.449	1.127	1.173	0.719	0.000
123789-HxCDF	0.041	0.086	0.023	0.024	0.111	0.280	0.295	0.187	0.000
1234678-HpCDF	0.401	0.811	0.209	0.237	1.054	2.700	2.846	1.819	0.000
1234789-HpCDF	0.064	0.140	0.036	0.041	0.176	0.449	0.489	0.294	0.000
OCDF	0.254	0.628	0.184	0.200	0.854	2.196	2.242	1.468	0.000
TCDD	2.702	5.445	2.253	6.050	11.115	9.993	8.355	5.984	0.004
PeCDD	2.086	3.907	1.441	3.474	7.098	8.425	7.761	4.977	0.000
HxCDD	1.652	3.734	1.090	3.321	6.365	8.957	8.394	5.029	0.000
HpCDD	1.086	2.228	0.497	1.570	3.440	6.544	6.543	3.542	0.001
OCDD	2.145	3.814	0.984	3.404	6.220	10.692	10.296	5.596	0.002
TCDF	1.463	3.161	0.944	0.929	4.078	9.414	9.569	6.041	0.006
PeCDF	1.399	2.939	0.828	0.819	3.805	9.529	9.566	6.233	0.004
HxCDF	1.166	2.508	0.673	0.700	3.239	8.344	8.667	5.467	0.003
HpCDF	0.698	1.536	0.384	0.437	1.944	5.007	5.371	3.360	0.001
OCDF	0.254	0.628	0.184	0.200	0.854	2.196	2.242	1.468	0.000

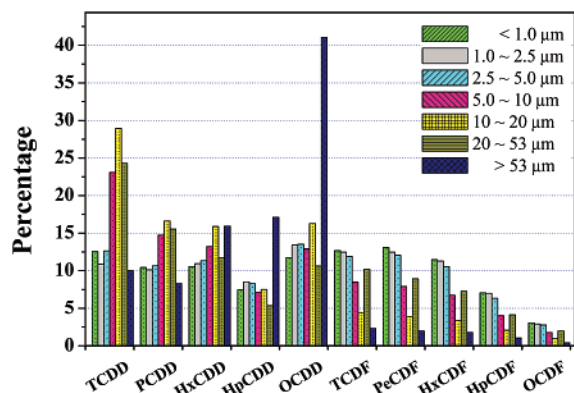


FIGURE 7. Normalized homologue profiles of total PCDD/Fs compared for each different size fraction.

As is shown in Figure 8(b), the P[2] score of low chlorinated dioxins was high, whereas that of the low chlorinated furans was low. Therefore, while particle fractions larger than 5.0  $\mu\text{m}$  are clustered into group I, which has dominant lower chlorinated dioxins, fractions smaller than 5.0  $\mu\text{m}$  are clustered into group II with dominant lower chlorinated furans. However, these distinguishable homologue patterns according to particle size in this study were somewhat different from other studies (13, 14). This may originate from different incineration conditions, incinerator type, and other factors (14). Since the current work is mainly focused on demonstrating joined analytical technique for determining size dependent level of toxic materials, a thorough examination has not been undertaken. In addition, while this work shows the size dependent distribution of PCDD/Fs contained in fly ash particles, it represents the dioxin distribution of the insoluble solid particles rather than that of total fly ash particles. Further studies of various types of fly ash samples are needed in order to develop detailed information on homologue patterns according to particle sizes.

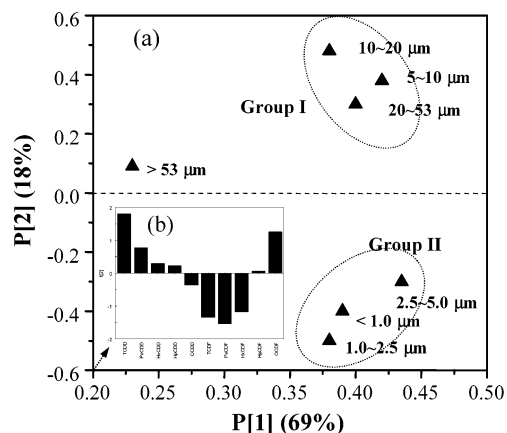


FIGURE 8. (a) Loading plot of principal component analysis for differently sized fractions of fly ash sample collected from MSWI. (b) P[2] score plot of principal component analysis.

In conclusion, the gravitational SPLITT fractionation technique has been used to make fine separations of fly ash, collected from a bag-filter house of incinerator, into different sized particles and was eventually used for obtaining size dependent levels of PCDD/Fs. The combined employment of GSF with any secondary analytical technique such as HRGC/HRMS demonstrates that it is a potential analytical method for obtaining size dependent information of particulate materials from the environment in relation to their production processes, chemical compositions, environmental fates, and other such factors. It is expected that the potential method introduced in this work will be applied to other particulate materials such as water sediments, airborne particles, and etc.

**Acknowledgments**

This study was supported by the grant No. 1999-2-124-001-5 from the Basic Research Program of the Korea Science & Engineering Foundation.

## Literature Cited

- (1) Schatowitz, B. *Chemosphere* **1994**, *29*, 2005–2013.
- (2) Fiedler, H. *Chemosphere* **1996**, *32*, 55–64.
- (3) Alcock, R. E.; Jones, K. C. *Environ. Sci. Technol.* **1996**, *30*, 3133–3143.
- (4) Chang, M. B.; Huang, T. F. *Chemosphere* **1999**, *39*, 2671–2680.
- (5) Domingo, J. L.; Schuhmacher, M.; Müller, L.; Riviera, J.; Granero, S.; Llobet, J. M. *J. Hazard. Mater.* **2000**, *76*, 1–12.
- (6) Schuhmacher, M.; Granero, S.; Riviera, J.; Müller, L.; Llobet, J. M.; Domingo, J. L. *Chemosphere* **2000**, *40*, 593–600.
- (7) Valberg, P. A.; Drivas, P. J.; McCarthy, S.; Watson, A. Y. *J. Hazard. Mater.* **1996**, *47*, 205–227.
- (8) Oh, J.-E.; Lee, K.-T.; Lee, J. W.; Chang, Y.-S. *Chemosphere* **1999**, *38*, 2097–2108.
- (9) Domingo, J. L.; Schuhmacher, M.; Llobet, J. M.; Müller, L.; Riviera, J. *Chemosphere* **2001**, *43*, 217–226.
- (10) Addink, R.; Antonioli, M.; Olie, K.; Govers, H. A. J. *Environ. Sci. Technol.* **1996**, *30*, 833–836.
- (11) Shin, K.-J.; Chang, Y.-S. *Chemosphere* **1999**, *38*, 2655–2666.
- (12) Chang, M.-B.; Chung, Y. U. *Chemosphere* **1998**, *36*, 1959–1968.
- (13) Clement, R. E.; Karasek, F. W. *J. Chromatogr.* **1982**, *234*, 395–405.
- (14) Karasek, F. W.; Clement, I. E.; Viau, A. C. *J. Chromatogr.* **1982**, *239*, 173–180.
- (15) Kaupp, H.; McLachlan, M. S. *Atmos. Environ.* **1998**, *31*, 85–95.
- (16) Kaupp, H.; McLachlan, M. S. *Atmos. Environ.* **2000**, *34*, 73–83.
- (17) Smith, R. L.; Davis, J. M.; Speckman, P. *Novart. Fdn. Symp.* **1999**, *220*, 59–97.
- (18) Donaldson, K.; MacNee, W. *Int. J. Hyg. Environ. Heal.* **2001**, *203*, 411–415.
- (19) Praelow, T. C.; Praelow, T. P. *Cell Biophys.* **1979**, *1*, 195–210.
- (20) Giddings, J. C. *Sep. Sci. Technol.* **1985**, *20*, 749–768.
- (21) Giddings, J. C. *Sep. Sci. Technol.* **1992**, *27*, 1489–1504.
- (22) Fuh, C. B.; Myers, M. N.; Giddings, J. C. *Anal. Chem.* **1992**, *64*, 3125–3132.
- (23) Gupta, S.; Ligrani, P. M.; Myers, M. N.; Giddings, J. C. *J. Microcolumn Sep.* **1997**, *9*, 213–223.
- (24) Fuh, C. B. *Anal. Chem.* **2000**, *72*, 266A–271A.
- (25) Moon, M. H.; Kang, D. J.; Lee, D. W.; Chang, Y. S. *Anal. Chem.* **2001**, *73*, 693–697.
- (26) Instrument Manual for Series SF1000 SPLITT Particle Separator, Version 1, FFFractionation, Salt Lake City, UT, 1997.

Received for review July 18, 2001. Revised manuscript received July 15, 2002. Accepted July 22, 2002.

ES011145O